ResearchGate

See discussions, stats, and author profiles for this publication at: https://www.researchgate.net/publication/255060339

ENDOR-determined solvation structure of VO/sup 2 +/ in frozen solutions

ARTICLE

CITATION
1

READS
338

2 AUTHORS, INCLUDING:

Devkumar Mustafi
University of Chicago
74 PUBLICATIONS **758** CITATIONS

SEE PROFILE

Available from: Marvin William Makinen
Retrieved on: 03 February 2016

dation, and the donors of the Petroleum Research Fund, administered by the American Chemical Society.

Supplementary Material Available: Heavy-atom compositions of the molecular orbitals of $C_2B_4H_6^{2-}$ (Table 1S), composition of molecular orbitals of $SnC_2B_4H_6$ (Table 2S), calculated Mulliken charges and Δ for substituents on $SnC_2B_4H_3R_3$ (Table 3S), composition of the molecular orbitals of $(C_{10}H_8N_2)SnC_2B_4H_6$ (Table 4S), and Mulliken overlap populations for $(C_{10}H_8N_2)SnC_2B_4H_6$ (Table 5S) (5 pages). Ordering information is given on any current masthead page.

Contribution from the Department of Biochemistry and Molecular Biology, Cummings Life Science Center, The University of Chicago, 920 East 58th Street, Chicago, Illinois 60637

ENDOR-Determined Solvation Structure of VO^{2+} in Frozen Solutions[1]

Devkumar Mustafi and Marvin W. Makinen*

Received October 16, 1987

The solvation structure of the vanadyl ion (VO^{2+}) in methanol and in water-methanol mixtures has been investigated by application of ^1H and ^{13}C electron nuclear double resonance (ENDOR) spectroscopy. The ligand origins of the proton ENDOR resonances have been assigned with use of materials selectively enriched with ^2H. The principal hyperfine coupling (hfc) components of both ^1H and ^{13}C in solvent molecules coordinated to the VO^{2+} ion have been determined by analysis of the $\mathbf{H}_0$ dependence of the ENDOR spectra. The hfc components of ^1H and ^{13}C of both metal-bound water and methanol exhibit axial symmetry. Under the point-dipole approximation the anisotropic hfc components yield estimates of the separation between the paramagnetic center and the ^1H and ^{13}C nuclei of axially and equatorially bound solvent molecules. Axially coordinated H_2O molecules exhiibit metal-proton distances of 2.92 and 3.42 Å, respectively, corresponding to an inner-sphere coordination site on one side of the equatorial plane and to a site with hydrogen bonding to the V=O group on the other side. Equatorially coordinated H_2O molecules exhibit metal-proton distances of 2.60 and 4.80 Å, corresponding to an inner-sphere coordination site and a hydrogen-bonded outer-sphere coordination site. In pure methanol there are similarly inner-sphere- and outer-sphere-bound methanol molecules in equatorial and axial positions, and the coordination structure determined on the basis of the metal-proton distances is confirmed by ENDOR spectroscopy with ^{13}C-enriched methanol. The ENDOR results provide unambiguous evidence that in water-methanol mixtures only $VO(H_2O)_5^{2+}$ and $[VO(H_2O)_4(CH_3OH)]^{2+}$ species are formed. In pure methanol the $VO(CH_3OH)_5^{2+}$ species is observed. The coordination geometries of the VO^{2+} complexes are deduced from ENDOR estimates of metal-nucleus distances by using computer-based molecular graphics. It is shown on the basis of molecular modeling that the ENDOR-determined metal-nucleus distances are best accounted for by complexes of tetragonal-pyramidal geometry.

Introduction

Complexes of the vanadyl ion (VO^{2+}) are stable and magnetically well-behaved and have been employed widely in spectroscopic studies. Although it is generally accepted that the VO^{2+} ion exists as a pentaaquo-hydrated species in solution, the actual composition of the complex has not been demonstrated. The structure of the $VO(H_2O)_5^{2+}$ species was first formulated for the complex in aqueous solution on the basis of its electronic absorption spectrum,[2] modeled according to the square-pyramidal geometry of the pentacoordinate complex of VO^{2+} with acetylacetonate[3] and of $VO(H_2O)_4(SO_4)\cdot H_2O$ in crystals.[4] While nuclear magnetic resonance studies with use of oxygen-17-enriched water identified dipolar interactions within the complex of the solvated VO^{2+} ion that could be ascribed to equatorial V···OH_2 interactions,[5] dipolar couplings could not be unambiguously assigned to an axial H_2O molecule.[6] Furthermore, the original X-ray study of $VO(H_2O)_4SO_4\cdot H_2O$ was analyzed only on the basis of Patterson projections[4,7] and the completed refinement of the crystallographic parameters determined in the subsequent study of Ballhausen, Djurinskij, and Watson[8] has not been reported. The structure analysis, thus, remains incomplete. Moreover, the $VO(H_2O)_5^{2+}$ species has not been observed hitherto in any crystal environment.

Since the first demonstration of electron nuclear double resonance[9] (ENDOR[10]), it has been used widely to characterize paramagnetic sites in solids and liquids. The electron spin of the paramagnetic site interacts with magnetic nuclei in its nearby environment through dipolar and contact interactions, producing shifts in their resonance frequencies. The dipolar interaction depends on the relative position of the nuclear spin with respect to the unpaired spin. ENDOR spectra of solid samples, obtained by partially saturating an EPR transition and sweeping a radio-frequency field through nuclear resonance transitions, can be analyzed to yield the dipolar contributions and to determine nuclear coordinates. Application of the theoretical equations relating the magnetic couplings of the **g** matrix and the hf interaction matrix to the set of molecular orientations selected for nuclear resonance in an ENDOR experiment becomes particularly straightforward in the case of paramagnetic sites of low g anisotropy,[11] as is the case for the VO^{2+} ion. We have employed ENDOR spectroscopy to determine the coordination environment of the Gd^{3+} ion[12] and to assign the conformation of nitroxyl

(1) This work was supported by grants from the National Institutes of Health (GM 21900 and AA 06374).
(2) Ballhausen, C. J.; Gray, H. B. *Inorg. Chem.* **1962**, *1*, 111-122.
(3) Dodge, R. P.; Templeton, D. H.; Zalkin, A. *J. Chem. Phys.* **1961**, *35*, 55-67.
(4) Palma-Vittorelli, M. B.; Palma, M. U.; Palumbo, D.; Sgarlata, F. *Nuovo Cimento* **1956**, *3*, 718-730.
(5) (a) Wüthrich, K.; Connick, R. E. *Inorg. Chem.* **1967**, *6*, 583-590. (b) Reuben, J.; Fiat, D. *Inorg. Chem.* **1969**, *8*, 1821-1824.
(6) Reuben, J.; Fiat, D. *Inorg. Chem.* **1967**, *6*, 579-583.
(7) The use of computers in reduction and full-matrix least-squares refinement of X-ray data was not then common practice. Thus, although the coordination structure deduced by Palma-Vittorelli et al.[4] yields distorted bonding relationships, it cannot be considered as erroneous without least-squares refinement of the atomic coordinates and temperature factors derived from the X-ray intensity data.
(8) Ballhausen, C. J.; Djurinskij, B. F.; Watson, K. J. *J. Am. Chem. Soc.* **1968**, *90*, 3305-3309.
(9) (a) Feher, G. *Phys. Rev.* **1956**, *103*, 834-835. (b) Feher, G. *Phys. Rev.* **1959**, *114*, 1219-1244.
(10) The following abbreviations are used: ENDOR, electron nuclear double resonance; EPR, electron paramagnetic resonance; hf, hyperfine; hfc, hyperfine coupling; rf, radio frequency.
(11) (a) Hurst, G. C.; Henderson, T. A.; Kreilick, R. W. *J. Am. Chem. Soc.* **1985**, *107*, 7294-7299. (b) Henderson, T. A.; Hurst, G. C.; Kreilick, R. W. *J. Am. Chem. Soc.* **1985**, *107*, 7299-7303.
(12) (a) Yim, M. B.; Kuo, L. E.; Makinen, M. W. *J. Magn. Reson.* **1982**, *46*, 247-256. (b) Yim, M. B.; Makinen, M. W. *J. Magn. Reson.* **1986**, *70*, 89-105.

0020-1669/88/1327-3360$01.50/0 © 1988 American Chemical Society

spin-labeled fluoroanilides and amino acids[13] in frozen solutions with accuracy approaching that obtained by diffraction techniques. Comparable ENDOR studies, but with relatively less emphasis on accuracy of structural detail, have been reported for frozen solutions of the *p*-benzoquinone anion radical,[14] Schiff base[15a] and imidazole[15b] complexes of VO^{2+} and of low-spin Co^{2+},[16] and a polycrystalline sample of bis(2,4-pentanedionato)copper(II).[11b]

In this paper we report the solvation structure of the VO^{2+} ion in frozen solutions of methanol and water–methanol mixtures on the basis of ^1H and ^{13}C ENDOR spectroscopy. The ENDOR spectra show that the $VO(CH_3OH)_5^{2+}$ species is formed in pure methanol, while in water–methanol mixtures both $VO(H_2O)_5^{2+}$ and $[VO(H_2O)_4(CH_3OH)]^{2+}$ species are present. We identify solvent molecules in both inner- and outer-sphere coordination sites, and the results provide unambiguous evidence for an axial, inner-sphere-coordinated solvent molecule. We show that the coordination structure is best accounted for by a complex of tetragonal-pyramidal geometry that can be constructed on the basis of ENDOR data with only the assumption of axial symmetry as specified by the **g** matrix that characterizes the VO^{2+} ion in frozen solutions.[17] The structural detail calculated on the basis of hf splittings to assign molecular geometry approaches the accuracy generally associated with X-ray crystallographic studies.

Experimental Methods

Vanadyl sulfate hydrate and methyl alcohol (99.9% spectrophotometric grade) were purchased from Aldrich Chemical Co., Inc. (Milwaukee, WI 53233); ^{13}C-enriched CH_3OH (99.7%) and D_2O (99.8%), from Sigma Chemical Co. (St. Louis, MO 63178). The deuteriated compounds CD_3OD (99.5%), CD_3OH (99%), and CH_3OD (99%) were obtained from Cambridge Isotope Laboratories, Inc. (Woburn, MA 01801). For EPR and ENDOR studies, the final metal ion concentration was 0.025 M in methanol or in a 50:50 (v/v) methanol–water cosolvent mixture. Deionized, distilled water was used throughout, and solutions were purged with nitrogen gas and stored frozen in EPR sample tubes to prevent oxidation.

EPR and ENDOR spectra were recorded with a Bruker ER 200D spectrometer equipped with an Oxford Instruments ESR10 liquid-helium cryostat and a Bruker digital ENDOR accessory, as previously described.[12] Typical experimental conditions for ENDOR measurements were as follows: sample temperature, 5 K; microwave frequency, 9.46 GHz; incident microwave power, 6.4 mW; rf power, 70 W with 12.5-kHz frequency modulation of the rf field. We estimate under these conditions for the cylindrical Bruker ENDOR cavity that $H_1 \simeq 0.04$ G and $H_2 \simeq 1.5$ G in the rotating frame according to studies reported by others[18] for this instrument. In general, a modulation depth of the rf field of no more than 10–30 kHz was used to record ENDOR spectra in order to ensure that the ENDOR line widths were not distorted. No modulation of the static laboratory magnetic field was used for recording ENDOR spectra.

Molecular modeling of the structures of solvated complexes of the VO^{2+} ion was carried out with use of the program SYBYL[19] running on an Evans and Sutherland PS330 molecular graphics system with a host Digital VAX 11/750 computer.

Results and Discussion

A. EPR Spectra of VO^{2+} Complexes. The V^{4+} ion has a $3d^1$ configuration. Since the orbital angular momentum is quenched by the crystalline field, the paramagnetism of the vanadyl ion has origin in spin angular momentum only. For rapidly tumbling complexes of the vanadyl ion in solution at room temperature, eight EPR transitions are observed because of the ($I = {}^7/_2$) vanadium nucleus. In frozen solutions the VO^{2+} ion has an axially symmetric **g** matrix and exhibits eight parallel and eight perpendicular absorption lines.[17,20]

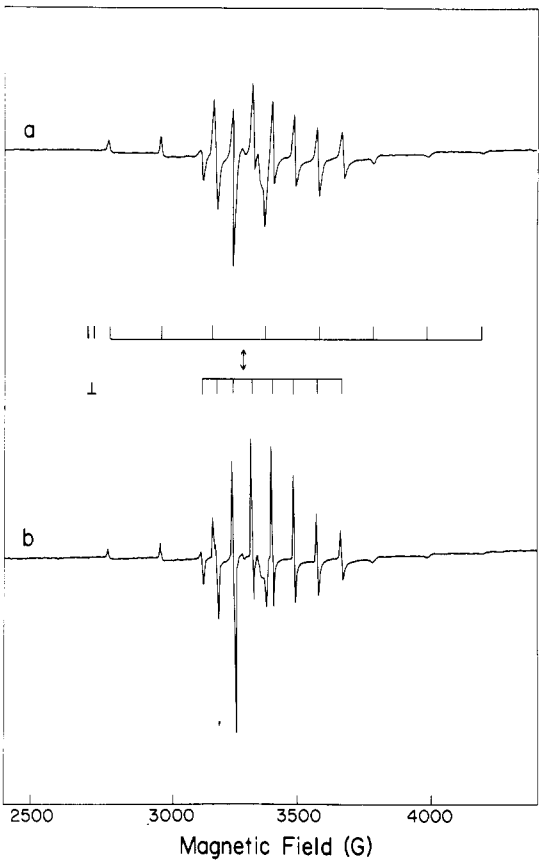

Figure 1. First-derivative EPR absorption spectra of VO^{2+} in (a) 50:50 (v/v) CH_3OH–H_2O and (b) 50:50 CD_3OD–D_2O solvent mixtures. The spectra were recorded as described under Experimental Methods with the samples at 15 K and with 83.4 μW of incident microwave power modulated at 12.05 kHz. The modulation amplitude was 1.25 G_{pp}. The parallel (||) and perpendicular ($\perp$) EPR absorption components ($-7/2$, $-5/2$, ..., $5/2$, $7/2$) are identified in sequence in the low- to high-field direction. The double-headed arrow indicates the magnetic field position corresponding to forbidden $\Delta M = \pm 1$ transitions.[20]

EPR absorption spectra of the VO^{2+} ion in water–methanol cosolvent mixtures are shown in Figure 1 for natural abundance and perdeuteriated cosolvent mixtures. There is a marked reduction in line width upon introduction of the perdeuteriated solvent mixture. The extent of the decrease is most accurately assessed for the $-3/2$ $\perp$ component of the spectrum, which appears as a well-separated resonance line. The decrease in the line width of the $-3/2$ $\perp$ resonance absorption feature upon introduction of perdeuteriated solvents is approximately 5.75 G. This is comparable to that of 6.15 G for transfer of the VO^{2+} ion from H_2O–glycerol to D_2O–glycerol mixtures.[17,20b] A similar spectrum was observed for VO^{2+} dissolved in neat methanol. For VO^{2+} dissolved in pure methanol, the decrease in line width of the $-3/2$ $\perp$ component corresponds to 3.62 G upon introduction of perdeuteriated methanol. There are four H_2O molecules coordinated to the VO^{2+} ion in equatorial positions in aqueous mixtures.[5] However, in pure methanol these positions can be occupied only by the hydroxyl group of the methanol molecule. The smaller decrease in line width for the VO^{2+} ion in pure, perdeuteriated methanol is, thus, consistent with the change in the stoichiometry of protons of the coordinated hydroxyl groups.

B. The Solvation Structure of VO^{2+} in Methanol. 1. Proton ENDOR Spectroscopy and Assignment of Hyperfine Coupling

(13) (a) Wells, G. B.; Makinen, M. W. *J. Am. Chem. Soc.* **1988**, *110*, 6343–6352. (b) Mustafi, D.; Wells, G. B.; Sachleben, J. R.; Makinen, M. W., manuscript in preparation.
(14) (a) O'Malley, P. J.; Babcock, G. T. *J. Chem. Phys.* **1984**, *80*, 3912–3913. (b) O'Malley, P. J.; Babcock, G. T. *J. Am. Chem. Soc.* **1986**, *108*, 3995–4001.
(15) (a) Attanasio, D. *J. Phys. Chem.* **1986**, *90*, 4952–4957. (b) Mulks, C. F.; Kirste, B.; van Willigen, H. *J. Am. Chem. Soc.* **1982**, *104*, 5906–5911.
(16) Baumgarten, M.; Lubitz, W.; Winscom, C. J. *Chem. Phys. Lett.* **1987**, *133*, 102–108.
(17) (a) Chasteen, N. D. *Coord. Chem. Rev.* **1977**, *22*, 1–36. (b) Chasteen, N. D. *Struct. Bonding (Berlin)* **1983**, *53*, 105–138.
(18) (a) Biehl, R. EPR Application Brief No. G565-9032-1, 1983; IBM Instruments, Inc., Danbury, CT 06810. (b) Brustolon, M.; Cassol, T.; Michelitti, L.; Segre, J. *Mol. Phys.* **1986**, *57*, 1005–1014.
(19) Marshall, G. B., personal communication. Detailed information on this program package can be obtained from Tripos Associates, Inc., 6548 Clayton Road, St. Louis, MO 63117.
(20) (a) Gersmann, H. R.; Swalen, J. D. *J. Chem. Phys.* **1962**, 3221–3233. (b) Albanese, N. F.; Chasteen, N. D. *J. Phys. Chem.* **1978**, *82*, 910–914.

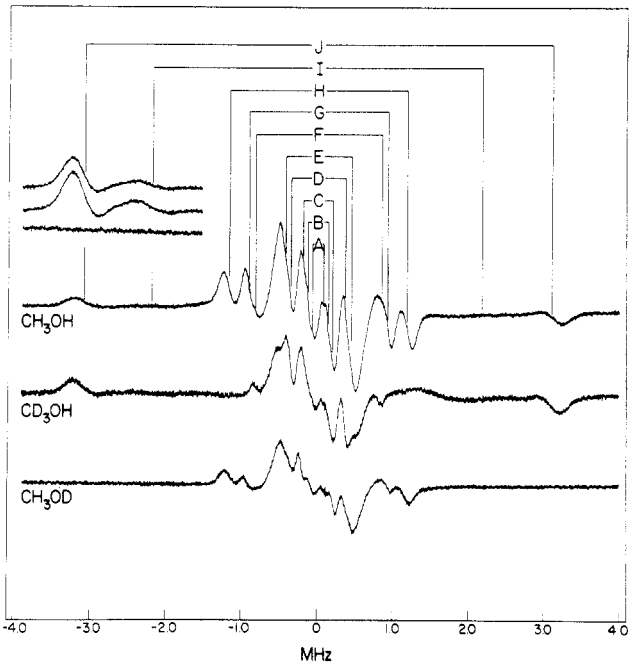

Figure 2. Proton ENDOR spectra of the VO^{2+} ion in methanol. $\mathbf{H}_0$ was set at the $-7/2 \parallel$ EPR resonance feature (~2800 G). The samples were prepared in CH_3OH, CD_3OH, and CH_3OD solvents. The ENDOR absorption features are identified in the stick diagram and are equally spaced about the free-proton frequency of 11.88 MHz. The line pairs are identified in Tables I and II. For ENDOR features near the free-proton frequency, a modulation depth no greater than 30 kHz of the rf field was required to achieve maximum spectral resolution. The spectra at apparent higher gain in the upper left-hand part were recorded with a modulation depth of approximately 90 kHz.

Components. ENDOR spectroscopy is performed at fixed magnetic field strength $\mathbf{H}_0$ by observing changes in the EPR signal intensity caused by nuclear transitions induced through sweeping the sample with an applied rf field. In the general case, the ENDOR transition frequencies are functions of the relative orientations of molecules with respect to $\mathbf{H}_0$, the electron–nucleus separation, the extent of anisotropy in the **g** matrix, and the relative orientations of the principal magnetic axes of the **g** matrix and the hf interaction matrix. For systems of low g anisotropy, as for the VO^{2+} ion in frozen solutions,[17,20] the first order ENDOR transition frequencies $\nu_\pm$ within the strong-field approximation are given by eq 1, in which $\nu_\pm$ represents the spacing of a pair

$$\nu_\pm = \nu_n \pm |A|/2 \qquad (1)$$

of ENDOR features that appear symmetrically about the free nuclear frequency ν_n and A represents an orientation-dependent hf coupling. Under the condition that $\mathbf{H}_0$ is applied parallel to the principal axis i of the hf interaction matrix, this becomes identical with the corresponding principal hfc component A_{ii}. The separation of $\nu_\pm$ about ν_n is called the ENDOR shift, and for symmetric separations the hf coupling is, thus, twice the value of this frequency spacing.

The EPR spectrum of the VO^{2+} ion is dominated by the hf anisotropy of the ($I = {}^7/_2$) vanadium nucleus. Application of $\mathbf{H}_0$ to the low-field ($-7/2 \parallel$) edge of the spectrum results in the single-crystal-type ENDOR spectra illustrated in Figure 2. The top spectrum exhibits ten pairs of ENDOR features. In the middle spectrum, corresponding to VO^{2+} in CD_3OH, seven pairs of resonance features due to hydroxyl protons are identified, and in the bottom spectrum, corresponding to VO^{2+} in CH_3OD, five pairs due to methyl protons are observed. Figure 3 illustrates the corresponding proton ENDOR spectra with $\mathbf{H}_0$ applied to the $-3/2$ $\perp$ resonance absorption line of the EPR spectrum. With this setting of $\mathbf{H}_0$, weak features were observed also at higher frequency, as shown in Figure 4. Comparison of the spectra in each figure shows that resonance features arising separately from methyl and hydroxyl protons frequently overlap. However, the chemical

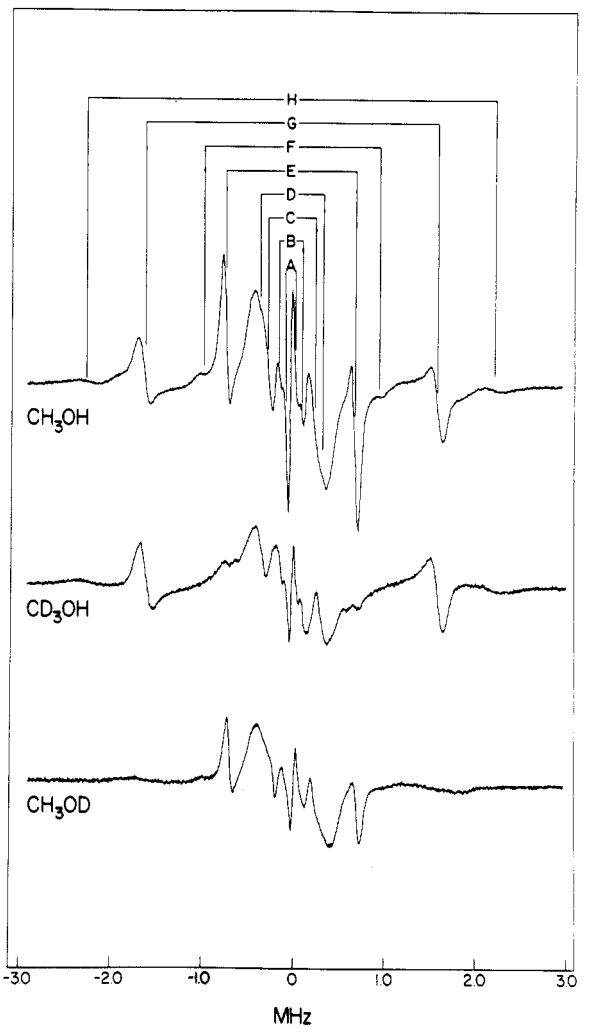

Figure 3. Proton ENDOR spectra of the VO^{2+} ion in methanol. $\mathbf{H}_0$ was set to the $-3/2$ $\perp$ EPR resonance feature (~3270 G). Eight line pairs are seen equally spaced about the free-proton frequency 13.88 MHz and are identified in Tables I and II. A modulation depth of 10 kHz of the rf field was required to achieve maximum spectral resolution. Other conditions are as in Figure 2.

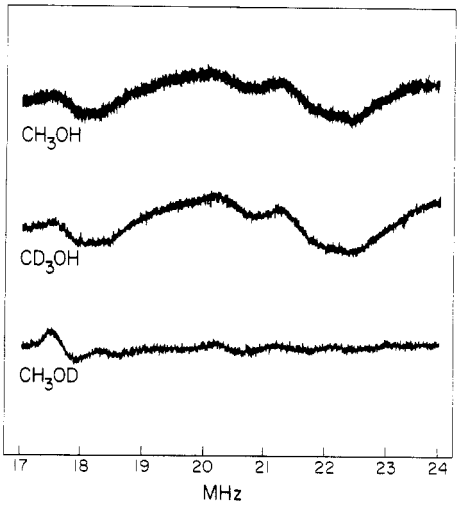

Figure 4. Proton ENDOR spectra of the VO^{2+} in methanol with the $\mathbf{H}_0$ setting at the $-3/2$ $\perp$ EPR resonance feature. These ENDOR lines observed at higher frequency are due to a much larger isotropic hfc component than for those in Figure 3. A modulation depth of 70 kHz of the rf field was employed. Other conditions are as in Figure 3.

origins and values of the splittings can be directly assessed on the basis of selective deuteriation. In Table I we have categorized from Figures 2–4 the various splittings according to chemical

Table I. Observed ENDOR Splittings of Hydroxyl Protons for the VO^{2+} Ion in Methanol

H_0 setting	line pair[a]	line splittings,[b] MHz	H_0 setting	line pair[a]	line splittings,[b] MHz
−7/2 ∥	A	0.121	−3/2 ⊥	A	0.120
	B	0.307		B	0.243
	D	0.728		D	0.700
	E	1.027		E	1.400
	F	1.642		G	3.214
	I	4.343		H	4.430
	J	6.120			
			−3/2 ⊥	*c*	7.611
				c	13.383
				c	15.668

[a] Line pairs are assigned in Figures 2 and 3. [b] Estimated uncertainty of the line splittings is ±0.007 MHz. [c] Line splittings are based on ENDOR features in Figure 4.

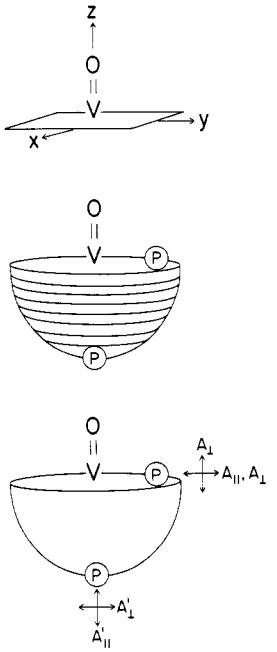

Figure 5. Schematic illustration of the relationships of the symmetry axes of the VO^{2+} ion to the principal axes of the **g** matrix and of the hf interaction matrix of nearby protons. The top diagram designates the direction of the molecular axes with respect to the V=O bond. The central diagram illustrates the relative positions of protons near the molecular *x,y* plane or near or on the symmetry *z* axis. Each circle represents the orientations of H_0 within the *g*-axis system that are selected according to nuclear position. The bottom diagram illustrates the principal hfc components that are detected for equatorially or axially positioned protons according to whether H_0 is aligned parallel or perpendicular to the *z* axis.

chemical origin and H_0 setting.

Our first objective is to identify the principal hfc components for each class of protons. Since the $g_\parallel$ component of the **g** matrix is coincident with the V=O bond and the $g_\perp$ components are coincident with the molecular *x,y* plane, application of H_0 at the −7/2 ∥ and −3/2 ⊥ EPR resonance absorption features should provide a means for selection of two different molecular orientations with correspondingly distinguishable hfc components. These conditions then should result in the observed hf couplings of protons schematically illustrated in Figure 5. The splittings can be classified into three categories: (1) splittings that are observed only for the parallel orientation of H_0; (2) splittings that are observed only for the perpendicular orientation of H_0; (3) splittings that are observed as common to both parallel and perpendicular spectra.

We first identify the principal hfc components of hydroxyl protons that are located along the molecular *z* axis. Because of the localization of the unpaired electron in the d_{xy} orbital of the V^{4+} ion,[17,20] the isotropic hfc contribution[21] may be expected to be small for hydroxyl protons located along the molecular *z* axis. On this basis, we conclude that the 6.12-, 3.21-, and 3.21-MHz splittings represent the most straightforward assignment of observed hfc components of an axially located hydroxyl proton since the 6.12- and 3.21-MHz splittings are prominently seen in only parallel and perpendicular orientations, respectively. Similarly, the 4.34- and 1.40-MHz splittings are ascribed to another type of axial hydroxyl proton. In contrast to the characteristics of axial protons, the observed splittings of hydroxyl protons located in the molecular *x,y* plane may be expected to have a large isotropic hfc contribution and will have hfc components common to both parallel and perpendicular spectra. With Figure 5 as a qualitative guide, these considerations are best answered by the 0.70-MHz splitting as the sharpest resonance line observed in both parallel and perpendicular spectra and by the 15.67-MHz splitting observed only in the perpendicular spectrum. We, thus, assign the 15.67-, 0.70-, and 0.70-MHz splittings as the observed hfc components of a class of hydroxyl protons located in the *x,y* plane. Similarly the 13.38-MHz feature is observed only in the perpendicular spectrum. The 1.03-MHz feature is observed in the parallel spectrum as well as in a series of ENDOR spectra with H_0 settings at intermediate values between the −7/2 ∥ and −3/2 ⊥ EPR transitions. However, in the perpendicular spectrum the 1.03-MHz feature is obscured by the nearby 1.4-MHz line that gains prominence in the spectrum when H_0 approaches the −3/2 ⊥ setting. On this basis, the 1.03-MHz feature must belong to a proton behaving similarly to that giving rise to the 0.70-MHz line. Therefore, we assign the observed 13.38- and 1.03-MHz splittings to another class of hydroxyl protons located in the *x,y* plane.

Comparable considerations were used to assign the principal hfc components of the methyl protons of coordinated methanol molecules on the basis of the orientation-dependent splittings summarized in Table II. For instance, the observed ENDOR splittings of 2.36 and 1.40 MHz in Table II are assigned to methyl protons along the molecular *z* axis, while the splittings of 3.21 and 1.96 MHz are assigned to methyl protons located in the molecular *x,y* plane. We have been unable to resolve resonances for the protons of the metal-bound methanol molecules presumably because of modulation conditions. Since we have resolved methyl protons by ENDOR spectroscopy in a variety of nitroxyl spin-labeled derivatives between temperatures of 40 and 90 K but with considerably less modulation (3–8 kHz),[13] we assume that methyl group rotation does not occur at 5 K and that the proton resonances are too broadened to be readily detected.

Table II. Observed ENDOR Splittings of Methyl Protons for the VO^{2+} Ion in Methanol

H_0 setting	line pair[a]	line, splittings,[b] MHz	H_0 setting	line pair[a]	line splittings,[b] MHz
−7/2 ∥	A	0.157	−3/2 ⊥	A	0.120
	C	0.414		B	0.243
	D	0.800		C	0.450
	G	1.828		D	0.700
	H	2.357		E	1.400
				F	1.957
				G	3.214

[a] Line pairs are assigned in Figures 2 and 3. [b] Estimated uncertainty of the line splittings is ±0.007 MHz.

2. Analysis of ENDOR Splittings and Estimation of Metal–Proton Distances. All of the ENDOR resonances observed for the VO^{2+} ion in methanol are accounted for in Figures 2–4, and the values of their splittings are tabulated in Tables I and II. Only

(21) There are two important contributions to isotropic hf coupling arising from (i) the Fermi contact interaction, which depends on the extent of covalency,[22] and (ii) the pseudocontact interaction,[23] which arises from the influence of ligands in adjoining coordination sites on the observed scalar coupling of a ligand nucleus. This latter term is proportional to the dipolar term multiplied by $\Delta g/g$ and is, thus, dependent on *g* anisotropy. In view of the low *g* anisotropy of the VO^{2+} ion with little change upon ligand substitution,[17,20] we conclude that the pseudocontact term is negligible and cannot be further distinguished here from the Fermi contact interaction.

Table III. Summary of Principal Hfc Components and Estimated Metal–Proton Distances of Hydroxyl Protons for the VO^{2+} Ion in Frozen Methanol[a]

$A_\parallel^{obs}$	$A_\perp^{obs}$	A_{iso}	$A_\parallel^{D}$	$A_\perp^{D}$	r, Å[b]	comment
6.12	3.21	−0.10	6.22	−3.11	2.90	axial OH
4.34	1.40	0.50	3.83	−1.91	3.42	V=O···H
15.67	0.70	4.76	10.91	−5.46	2.52	equatorial OH (in-plane)
13.38	1.03	3.77	9.61	−4.78	2.60	equatorial OH (out-of-plane)
1.64	0.31	0.34	1.30	−0.65	4.80	outer-sphere, axial OH
7.61	0.12	2.45	5.16	−2.57	3.20	outer-sphere, equatorial OH

[a] Hfc components are given in units of MHz. [b] Estimated error is ±0.1 Å.

Table IV. Summary of Prinicpal Hfc Components and Estimated Metal–Proton Distances of Methyl Protons for the VO^{2+} Ion in Frozen Solutions[a]

$A_\parallel^{obs}$	$A_\perp^{obs}$	A_{iso}	$A_\parallel^{D}$	$A_\perp^{D}$	r, Å[b]	comment
2.36	1.40	−0.15	2.51	−1.25	3.92	axial CH_3–
0.80	0.45	0.03	0.83	−0.42	5.60	V=O···$HOCH_3$
3.21	1.96	−0.23	3.44	−1.73	3.54	equatorial CH_3–
1.83	0.16	0.50	1.33	−0.66	4.85	outer-sphere, axial CH_3–

[a] Hfc components are given in units of MHz. [b] Estimated error is ±0.1 Å.

two pairs of features were identified for each class of protons. We conclude, therefore, that the principal hfc components for each class of protons exhibit axial symmetry. We assume that the experimentally observed ENDOR splittings arise predominantly fromm anisotropic dipolar interactions between the unpaired electron and protons and to a lesser extent from isotropic interactions.[21] This is represented by eq 2, where A^{obs} is the observed

$$A^{obs} = g_e|\beta_e|g_n|\beta_n|(3\cos^2\phi - 1)/hr^3 + A_{iso} \qquad (2)$$

splitting under the conditions described for eq 1 and A_{iso} is the isotropic hfc contribution due to both Fermi contact[22] and pseudocontact[23] interactions. Under the point-dipole approximation and within the strong-field limit, the anisotropic hfc contribution due to dipole–dipole interactions corresponds to the first term on the right-hand side of eq 2, where r is the modulus of the position vector $\mathbf{r}$ between the proton and the electron and ϕ is the angle between $\mathbf{r}$ and $\mathbf{H}_0$. In eq 2 g_e represents the effective g value defined by the relation $g_e = (g_\parallel^2\cos^2\theta + g_\perp^2\sin^2\theta)^{1/2}$ and θ describes the angle that $\mathbf{H}_0$ makes with the symmetry axis of the complex, β_e represents the Bohr magneton, and g_n and β_n are the nuclear g value and the nuclear magneton, respectively. The principal hfc components $A_\parallel$ and $A_\perp$ correspond to the observed splittings when $\phi = 0$ and 90°, respectively. Since the dipolar interaction is dominated by the unpaired electron on the metal ion, we assign the hfc component with the largest magnitude as positive, and the observed splittings are subject to the constraint $(A_\parallel + 2A_\perp)/3 = A_{iso}$. In Tables III and IV we have summarized our assignments of the principal dipolar and isotropic hfc components for each class of hydroxyl and methyl protons. In Tables III and IV we have also listed the metal–proton distances calculated according to eq 2 on the basis of the dipolar anisotropic hfc components and have added brief comments for each class of protons to indicate the structural relationships of the ligand to the VO^{2+} moiety. These data will be discussed in more detail below with respect to the results of molecular modeling studies.

In Table III there are three categories of hydroxyl protons that exhibit hfc interactions with the VO^{2+} ion and are ascribed to axially positioned, equatorially positioned, and outer-sphere OH groups. In general, the values of the isotropic contact terms are smaller for the outer-sphere-coordinated OH groups than for inner-sphere hydroxyl protons, and the largest isotropic hfc components are associated with equatorially located hydroxyl protons. In view of the low g anisotropy of the VO^{2+} ion and the observation[17,20b] that this anisotropy is little influenced by changes of ligands in equatorial positions, we conclude that the variations of A_{iso} in Table III are due primarily to the Fermi contact hf interaction. Our estimates of the isotropic hfc contribution for each class of protons are reasonable. The averaged isotropic contact term for H_2O molecules equatorially coordinated to VO^{2+} doped into crystals of $Mg(NH_4)_2(SO_4)_2{\cdot}6H_2O$ is 4.84 MHz[24] compared to our values of 3.77 and 4.76 MHz for the hydroxyl protons of equatorially coordinated methanol molecules. Also, the contribution of the Fermi contact term has been estimated at +3.2 MHz[5b] through proton-relaxation-enhancement studies of VO^{2+} in aqueous solutions. This represents essentially the scalar-coupling contributions of only equatorially bound water molecules. In view of the similar chemical bonding structure of the OH group in water and methanol, these estimates for the Fermi contact contribution of the VO^{2+} ion in water are in substantial agreement with the results in Table III.[25] Also, our estimate of the isotropic contribution of the inner-sphere, axially coordinated methanol molecule in Table III is in excellent agreement with that of −0.03 MHz for axially coordinated H_2O determined through single-crystal ENDOR studies of VO^{2+} doped into the host matrix of $Mg(NH_4)_2(SO_4)_2{\cdot}6H_2O$.[24] A rapidly exchanging solvent molecule with a Fermi contact term of +2 MHz has been observed by proton-relaxation enhancement and attributed to either the axially bound water molecule or to outer-sphere-bound water.[5,6] In view of the excellent agreement for isotropic hfc contributions described above between our results and those of others, the results in Table III suggest that the 2-MHz contribution observed[5,6] in nuclear magnetic resonance experiments could have origin in outer-sphere solvent molecules only.

On the basis of the ENDOR data, as indicated in Table III, there are two types of CH_3OH molecules coordinated to the VO^{2+} ion with hydroxyl protons located in a plane perpendicular to the molecular z axis. The metal–proton distances together with the geometry of the methanol molecule require that the oxygen atoms of the two types of equatorial CH_3OH ligands are 1.90 and 1.98 Å distant from the vanadium atom. These estimates are in good agreement with the range of V···O distances of 1.983–2.048 Å observed for the four equatorially positioned oxygen-donor ligands in $VO(H_2O)_4SO_4{\cdot}H_2O$.[8] The ENDOR absorptions for the pair of resonance features D in Figure 3 and the 15.668-MHz resonance feature in Figure 4, respectively, for the 2.52-Å proton are particularly narrow and well-defined, compared to those for the 2.60-Å proton. Also, they are readily seen as single-crystal-type resonance features with $\mathbf{H}_0$ in parallel and perpendicular orientations. We conclude on this basis that the 2.52-Å protons are

(22) Owen, J.; Thornley, J. H. M. In *Reports on Progress in Physics*; Strickland, A. C., Ed; The Physical Society: London, 1966, Vol. 29, pp 675–728.
(23) (a) McConnell, H. M.; Chestnut, D. B. *J. Chem. Phys.* **1958**, *28*, 107–117. (b) McConnell, H. M.; Robertson, R. E. *J. Chem. Phys.* **1958**, *29*, 1361–1365.
(24) Atherton, N. M.; Shakelton, J. F. *Mol. Phys.* **1980**, *39*, 1471–1485.
(25) The only related magnetic resonance study, to our knowledge, of the VO^{2+} in pure methanol is that of Angerman and Jordan.[26] However, their line-broadening studies do not provide a direct estimate of the Fermi contact contributions of coordinated methanol molecules.
(26) Angerman, H. S.; Jordan, R. B. *Inorg. Chem.* **1969**, *8*, 1824–1833.

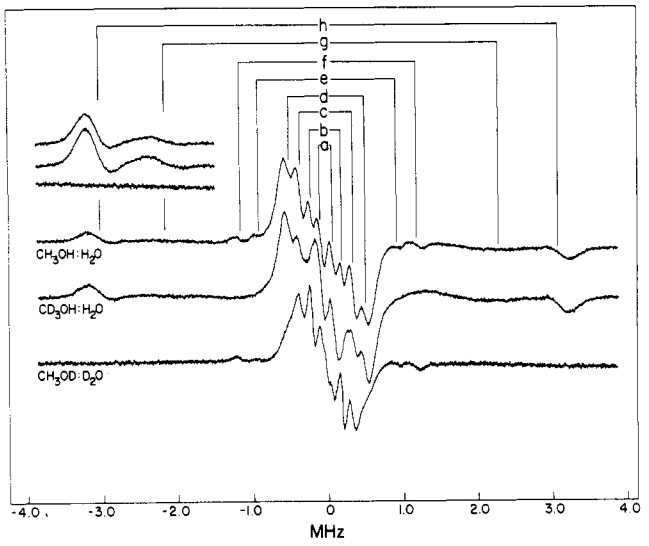

Figure 6. Proton ENDOR spectra of the VO^{2+} ion in 50% water–methanol. H_0 was set to the $-7/2$ || EPR absorption feature (~2800 G). The VO^{2+} complexes were prepared as indicated in the following 50:50 (v/v) solvent mixtures: CH_3OH–H_2O, CD_3OH–H_2O, and CH_3OD–D_2O. The ENDOR lines of each pair are identified in the stick diagram and are seen to be equally spaced about the free-proton frequency of 11.84 MHz. The line pairs are identified in Table V. Other conditions are as in Figure 2.

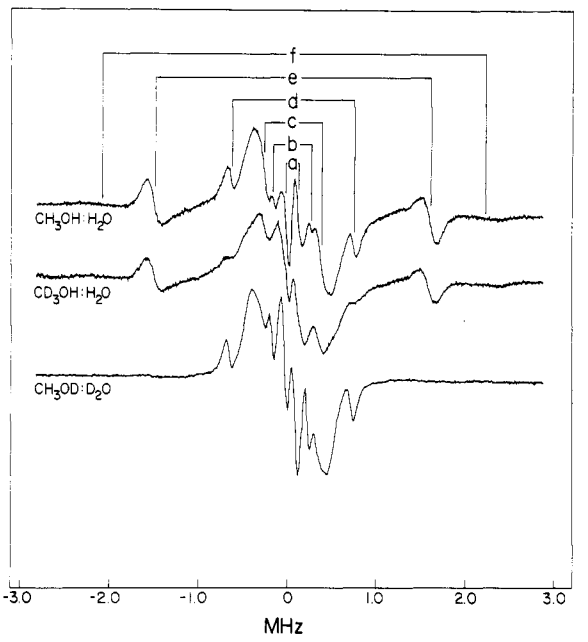

Figure 7. Proton ENDOR spectra of the VO^{2+} ion in 50% aqueous methanol. H_0 was set to the $-3/2$ ⊥ EPR absorption (~3270 G). Six line pairs are seen equally spaced about the free-proton frequency (13.88 MHz) and are identified in Table V. Other conditions are as in Figure 3.

uniformly located in the molecular x,y plane and exhibit a low degree of structural disorder. On the other hand, the other type of hydroxyl proton with the 2.60-Å distance exhibits broader ENDOR absorptions, indicating a greater degree of structural disorder. If this disorder were confined to variations of the OH group within the molecular x,y plane, the $A_\perp$ component would still remain sharply defined as for the other type of equatorial hydroxyl proton. We, therefore, conclude that the disorder arises from deviations of the hydroxyl proton out of the x,y plane.

The results in Table III also show that there are two types of axially positioned hydroxyl protons. We suggest that the one with a metal–proton distance of 2.90 Å belongs to a CH_3OH molecule located so that its oxygen atom lies on the molecular z axis. For an idealized H—O bond distance of 0.956 Å and a valence angle of 108.9° for the hydroxyl oxygen of the methanol molecule,[27] this geometry places the methanol oxygen 2.22 Å from the vanadium atom in a position trans to the V=O group and in a resultant collinear O···V=O configuration. The other axial CH_3OH molecule with a metal–proton distance of 3.42 Å, therefore, must lie so that it is hydrogen-bonded to the V=O group.

In Table IV metal–proton distances are given for methyl protons of VO^{2+}-coordinated methanol molecules. There are two types of axially positioned methyl protons. The metal–proton distance of 3.92 Å belongs to one type of CH_3OH molecule located along the molecular z axis. This distance, together with the observed (hydroxyl) metal–proton distance of 2.90 Å for one type of axial methanol molecule in Table III, places the methanol oxygen atom at a distance of 2.22 Å along the axis from the metal ion. Although there is no X-ray structure of a methanol-coordinated complex of VO^{2+}, the separation of the O atom of the corresponding axial water in $VO(H_2O)_4SO_4 \cdot H_2O$ is 2.23 Å.[8] A metal–proton distance of 5.60 Å is calculated for the methyl group of the second type of axially positioned methanol molecule. With a metal–OH distance of 3.42 Å, as shown in Table III for this axial hydrogen-bonded molecule, a V···O distance of 4.39 Å is calculated. With a V=O bond distance of 1.59 Å[8] and an H—O bond distance of 0.96 Å, the O(vanadyl)···O(methanol) distance is then 2.79 Å. This is nearly exactly the average O···O distance observed for hydrogen-bonded hydroxyl groups in water and alcohols.[27]

Table V. Observed ENDOR Splittings of Hydroxyl and Methyl Protons for the VO^{2+} Ion in Frozen Water–Methanol Cosolvent Mixtures[a,b]

H_0 setting	line pair[a]	line splittings,[b] MHz	H_0 setting	line pair[a]	line splittings,[b] MHz
		A. Hydroxyl Protons			
$-7/2$ ||	a	0.164	$-3/2$ ⊥	a	0.150
	c	0.700		c	0.680
	d	1.028		d	1.400
	g	4.343		e	3.086
	h	6.071		f	4.328
					7.611[c]
					13.383[c]
					15.668[c]
		B. Methyl Protons			
$-7/2$ ||	a	0.164	$-3/2$ ⊥	a	0.150
	b	0.407		b	0.414
	c	0.700		c	0.680
	e	1.871		d	1.40
	f	2.343			

[a] Line pairs are assigned in Figures 6 and 7. [b] Estimated uncertainty of the line splittings is ±0.007 MHz. [c] Data not shown; see text.

Metal–proton distances have been estimated for VO^{2+} in methanol on the basis of nuclear magnetic resonance line-broadening effects.[26] These results, however, are calculated for an assumed stoichiometry corresponding to $VO(CH_3OH)_5^{2+}$ and are averaged over the entire complex. The results were not analyzed for separate axial and equatorial interactions and, therefore, cannot be meaningfully compared to the results in Tables III and IV.

C. The Solvation Structure of VO^{2+} in Water–Methanol Cosolvent Mixtures. Figures 6 and 7 illustrate the proton ENDOR spectra of VO^{2+} dissolved in a 50:50 (v/v) water–methanol mixture with H_0 applied at the $-7/2$ || and $-3/2$ ⊥ EPR absorptions, respectively. Spectra are correspondingly compared with selectively deuteriated cosolvents. As in Figures 2 and 3, there are overlapping resonances due to hydroxyl and methyl protons that are resolvable on the basis of deuterium substitution. Similarly

(27) Ondik, H.; Smith, D. In *International Tables for X-ray Crystallography*, 2nd ed.; MacGillavery, C. H., Rieck, G. D., Eds.; Kymoch: Birmingham, England, 1968; Vol. III, pp 273–274.
(28) Pauling, L. Interatomic Distances and Their Relation to the Structure of Molecules and Crystals. *The Nature of the Chemical Bond*, 3rd ed.; Cornell University Press: Ithaca, NY, 1960; Chapter 7, pp 221–264.

Table VI. Summary of Principal Hfc Components and Estimated Metal–Proton Distances of Hydroxyl and Methyl Protons of VO^{2+} in Frozen Water–Methanol Mixtures[a]

$A_{\parallel}^{obs}$	$A_{\perp}^{obs}$	A_{iso}	$A_{\parallel}^{D}$	$A_{\perp}^{D}$	r, Å[b]	comment
6.07	3.09	−0.03	6.10	−3.06	2.92	axial OH
4.34	1.40	0.51	3.83	−1.91	3.42	V=O···H
15.67	0.70	4.76	10.91	−5.46	2.52	equatorial OH (in-plane)
13.83	1.03	3.77	9.61	−4.80	2.60	equatorial OH (out-of-plane)
7.61	0.16	2.40	5.19	−2.58	3.20	outer-sphere, equatorial OH
2.34	1.40	−0.15	2.50	−1.25	3.92	axial CH_3–
1.87	0.16	0.50	1.35	−0.68	4.84	outer-sphere, axial CH_3–
0.70	0.41	−0.04	0.74	−0.37	5.70	outer-sphere, equatorial CH_3–

[a] Hfc components are given in units of MHz. [b] Estimated error is ±0.1 Å.

Table VII. Summary of Principal Hfc Components of ^{13}C and Estimated Metal–Carbon Distances of VO^{2+} in Frozen Solutions of Methanol and in Water–Methanol Cosolvent Mixtures[a,b]

line pair in Figure 8	$A_{\parallel}^{obs}$	$A_{\perp}^{obs}$	A_{iso}	$A_{\parallel}^{D}$	$A_{\perp}^{D}$	r, Å	comment
b	0.987	0.439	0.036	0.951	−0.475	3.43	axial CH_3[c]
c	2.040	0.671	0.233	1.808	−0.904	2.78	equatorial CH_3
a	0.227	0.130	−0.011	0.238	−0.119	5.45	outer-sphere, equatorial CH_3
b′	0.986	0.428	0.043	0.942	−0.471	3.45	axial CH_3[c]
a′	0.272	0.159	−0.015	0.287	−0.144	5.12	outer-sphere, equatorial CH_3

[a] Line pairs are assigned in Figure 8; Hfc components are given in units of MHz. [b] Estimated uncertainties of the line splittings and distances are ±0.007 MHz and ±0.1 Å, respectively. [c] The $b_{\parallel}$ and $b'_{\parallel}$ ENDOR features are observed in the −7/2 ∥ spectrum (data not shown).

to the case for Figure 4, comparably broad resonance features were observed at higher frequencies for VO^{2+} in water–methanol mixtures (data not shown). We have summarized the values of the ENDOR splittings in Table V for the resolved features in Figures 6 and 7, including the splittings at higher frequencies.

In Table VI we have indicated the corresponding assignments for the hfc components of each class of protons. In general, the values of the hfc components and the calculated metal–proton distances are similar to those derived for the solvated VO^{2+} ion in pure methanol. However, close inspection of Figures 6 and 7 and Table VI shows that no resonances are observed for methyl protons of equatorially positioned, inner-sphere-coordinated CH_3OH molecules. To determine the origin of this difference, we have analyzed the ENDOR spectra of VO^{2+} in water–methanol mixtures of variable water concentration. While weak resonance features were observed for equatorial methyl protons in methanol mixtures with ~1% (v/v) H_2O, they were completely absent in mixtures containing ≥3–4% (v/v) H_2O. On this basis, we conclude that in aqueous cosolvent mixtures having more than 3% (v/v) H_2O there are no equatorially positioned CH_3OH molecules directly coordinated to the VO^{2+} ion. On the other hand, the ENDOR data provide unambiguous evidence for a CH_3OH molecule in an axial, inner-sphere coordination site of the VO^{2+} ion in 50:50 water–methanol mixtures. These observations indicate the presence of two populations of VO^{2+} complexes in water–methanol mixtures, one with axially coordinated H_2O and the other with axially coordinated methanol. Both types of complexes have only H_2O molecules coordinated in equatorial positions. No resonance features were observed with $\mathbf{H}_0$ applied at the −7/2 ∥ EPR line that could be attributed to the methyl protons of an axially positioned CH_3OH molecule hydrogen-bonded to the V=O group, as for the VO^{2+} ion in pure methanol. However, ENDOR splittings of methyl protons were observed that could be assigned to outer-sphere-coordinated CH_3OH. For the methyl protons designated as outer sphere in Table VI, the most prominent resonance features were observed in the −3/2 ⊥ spectrum, indicating that they are distributed about the equatorial plane.

D. Confirmation of Solvation Structure by ^{13}C ENDOR Spectroscopy. For purposes of confirming our assignment of the solvation structure of VO^{2+}, we have carried out similar experiments with ^{13}C-enriched methanol. Representative results are illustrated in Figure 8 in which the ^{13}C ENDOR spectra are presented for the VO^{2+} ion in pure methanol and in a 50:50 (v/v) methanol–H_2O cosolvent mixture. In Table VII we have summarized the values of the observed ENDOR splittings for each class of ^{13}C nuclei together with the corresponding assignments of principal hfc components. It is evident that the 2.04- and

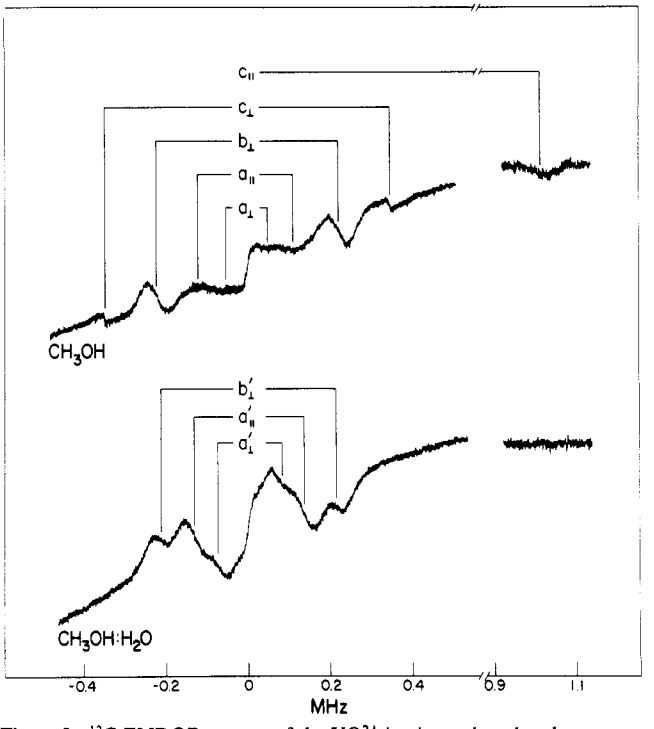

Figure 8. ^{13}C ENDOR spectra of the VO^{2+} ion in methanol and aqueous methanol mixtures. $\mathbf{H}_0$ was set to the −3/2 ⊥ EPR absorption. The lower frequency component belonging to line pair $c_{\parallel}$ was not detectable as expected in the 1.5–2.5-MHz region because of a severely sloping base line. For both types of solvent systems, methanol enriched to 50% mole fraction ^{13}C was employed to ensure that the relative enrichment of metal-bound methanol molecules remained constant. The modulation depth of the rf field was 30 kHz. Other conditions are as in Figure 3.

0.67-MHz splittings are observed for the VO^{2+} ion only in pure methanol. These pairs of resonance features are attributable to an equatorially positioned methyl group, and the calculated V···C distance of 2.78 Å assigns it to an inner-sphere-coordinated molecule. Correspondingly, the 0.987- and 0.439-MHz splittings observed for the complex in pure methanol identify an axially coordinated methanol molecule in an inner-sphere coordination site. The ENDOR spectra show that the resonances for the cosolvent mixture are considerably reduced in intensity. Nonetheless, they confirm that an axially coordinated methanol molecule obtains also in the cosolvent mixture although we are not able to estimate its relative occupancy. Because of the low

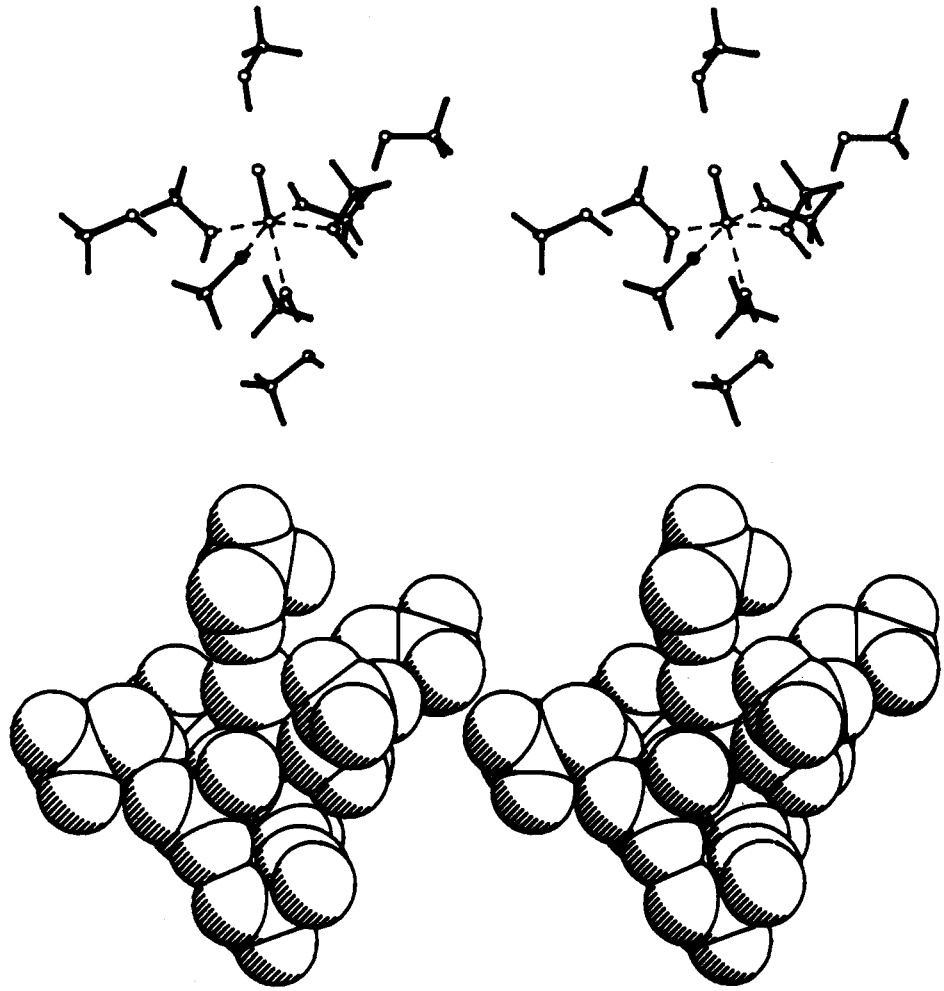

Figure 9. Stereodiagrams of the coordination structure of the VO^{2+} ion in methanol determined on the basis of ENDOR spectroscopy and molecular modeling. The upper diagram illustrates the complex in stick skeletal form. Broken lines connect the inner-sphere methanol molecules coordinated to the vanadium. The lower diagram illustrates the complex in space-filling form, in the same projection as in the upper diagram. The lower diagram is drawn to scale for van der Waals radii[27,28] of 1.53 Å (C), 1.4 Å (O), 1.2 Å (H), and 1.35 Å (V).

signal-to-noise ratio intrinsic to the collection of ^{13}C ENDOR spectra with our present spectrometer, resonance features could not be clearly resolved in either solvent system that were attributable to an axially positioned CH_3OH molecule hydrogen-bonded to the V=O group. As shown in Figures 2–4 and Tables I–III, this structural feature could be clearly assigned on the basis of ^1H ENDOR results.

The ^{13}C ENDOR spectra of the VO^{2+} ion in both solvent systems exhibit resonance features attributable to outer-sphere CH_3OH molecules distributed about the equatorial plane. However, while the line widths are comparable for both systems, the amplitudes of the resonances are greater for the VO^{2+} ion in the water–methanol mixture. Since the relative proportions of metal ion to ^{13}C nuclei were kept constant in these experiments, the greater amplitude indicates a higher density of outer-sphere CH_3OH molecules in the aqueous cosolvent mixture. Our ENDOR results have shown that in the cosolvent mixture only H_2O molecules are coordinated to the VO^{2+} ion in the equatorial plane. Both the greater density of outer-sphere-localized CH_3OH molecules and the somewhat shorter V···C separation for the VO^{2+} ion in the aqueous cosolvent mixture are, thus, consistent with the reduced steric volume that equatorially coordinated H_2O molecules would occupy.

The metal–carbon separation in Table VII calculated on the basis of ^{13}C ENDOR data agree to within ±0.3 Å with corresponding distances predicted on the basis of X-ray-defined metal–oxygen bond lengths.[8] As for the ^1H ENDOR results, there is a slightly greater discrepancy for metal–carbon distances of equatorially positioned methanol molecules when compared to expectations based on the X-ray-defined bond lengths. This is again due to the greater isotropic contact interactions that the equatorial molecules exhibit compared to axially positioned ligands.

E. Molecular Modeling of the Solvation Structure of the VO^{2+} Ion. We have examined the structural relationships of the inner-sphere- and outer-sphere-coordinated solvent molecules to each other in the VO^{2+} complexes to determine how accurately ENDOR-determined electron–nucleus distances are accommodated by nonbonding, van der Waals constraints. For the modeling studies, we have assumed only bond lengths and valence angles of idealized methanol and water molecules,[27] the V=O bond length of 1.59 Å determined in X-ray diffraction experiments,[8] and the requirement of an axially symmetric complex in accordance with the principal values of the **g** matrix.[17,20b] Because of the more demanding steric constraints of coordinated methanol molecules, we present only the modeling results of the solvation structure of the VO^{2+} ion in pure methanol, since separate modeling of the $VO(H_2O)_5^{2+}$ and the $[VO(H_2O)_4(CH_3OH)]^{2+}$ complexes remains compatible with the analysis of the $VO(CH_3OH)_5^{2+}$ species. The structure of the VO^{2+} ion in methanol with both inner-sphere- and outer-sphere-coordinated solvent molecules as determined by molecular modeling is illustrated in Figure 9.[29]

To deduce the solvation structure of the VO^{2+} ion, we first coordinated the oxygen of a methanol molecule so as to form a linear O···V=O configuration with the hydroxyl proton and methyl carbon 2.90 and 3.43 Å distant from the vanadium atom, respectively, according to the ENDOR results. These constraints then position the oxygen 2.22 Å distant from the vanadium, in excellent agreement with the X-ray-determined axial H_2O···V=O

(29) A listing of the molecular-graphics-derived atomic coordinates of the complex illustrated in Figure 9 will be provided upon written request.

distance of 2.23 Å.[8] The steric requirements of a methanol molecule allow only four inner-shell-coordinated molecules in equatorial positions. These were positioned so that the vanadium–oxygen bond vector bisects the C–O–H valence angle of each methanol molecule and the equatorial ligands are close-packed to the axially coordinated methanol. Both the ^1H and the ^{13}C ENDOR results indicate that the metal–nucleus distances for equatorially positioned hydroxyl protons and methyl carbon atoms are underestimated by ~0.1 and 0.3 Å, respectively, when compared to X-ray results.[8] This difference is due either to the stronger isotropic hfc of equatorially positioned ligands with the unpaired electron in the metal d_{xy} orbital or to breakdown of the strong-field approximation for the short electron–proton distances involved. This discrepancy represents the greatest error in our present study and is seen for both inner- and outer-sphere equatorial ligands. Therefore, the equatorial vanadium–oxygen bond length was adjusted to 2.04 Å on the basis of the X-ray structure of $VO(H_2O)_4SO_4 \cdot H_2O$[8]. The requirement of the equatorially positioned ligands as closely packed to the axially bound methanol molecule is sufficient to fix the O=V—O angle with equatorial oxygens at 97.9°, in exact agreement with X-ray results.[8] The steric volumes of the four equatorially positioned methanol molecules prevent a binding geometry with all four methyl groups simultaneously in, above, or below the molecular x,y plane. We, therefore, positioned two methyl groups of trans-coordinated molecules above the plane with the other two positioned below the plane. This conformation permits two equatorial hydroxyl protons to lie exactly in the molecular x,y plane ($\angle$O=V···H = 90°) while the other two lie below the x,y plane ($\angle$O=V···H = 115°). This arrangement is, thus, in agreement with the sets of narrow and broad resonances observed in the ENDOR spectra for two types of equatorially positioned hydroxyl protons.

With the inner coordination shell fixed, we then searched for plausible sites of outer-sphere-bound methanol molecules that could account for the ENDOR data. The axially positioned methanol molecule hydrogen-bonded to the vanadyl oxygen was fixed according to the ENDOR-determined metal–proton distance of its hydroxyl group and the average metal–proton distance to the methyl group. In particular, the vanadium–(hydroxyl) proton distance determined by ENDOR spectroscopy yields a D–H···A distance for hydrogen bonding that is in excellent agreement with expectation. The remaining, outer-sphere-located methanol molecules were positioned according to van der Waals nonbonded constraints imposed by the inner-sphere ligands, steric accommodation of closely packed, outer-sphere molecules, and metal–nucleus distances in reasonable agreement with ENDOR results. These considerations allow plausible binding sites for two symmetry-related, equatorially positioned, outer-sphere methanols and one axially located outer-sphere molecule on the side of the molecular x,y plane opposite from the vanadyl oxygen. As a result of these modeling constraints, the outer-sphere molecules each have orientations that place their hydroxyl groups according to D–H···A distance and angle into plausible hydrogen-bonding interactions with inner-sphere-located methanol oxygen atoms. These interactions could conceivably stabilize the outer-sphere-bound methanol molecules. The ENDOR results provide direct evidence for outer-sphere-bound solvent molecules also in water–methanol mixtures. Their metal–proton distances indicate that they would be similarly stabilized through hydrogen-bonding interactions.

Contribution from the Laboratory of Analytical Chemistry, Faculty of Science, Nagoya University, Nagoya 464-01, Japan

Dilatometric Studies on Reaction Volumes for the Formation of Nickel(II) Complexes in Aqueous Solution

Toru Amari, Shigenobu Funahashi, and Motoharu Tanaka*

Received December 9, 1987

Reaction volumes for the formation of nickel(II) complexes with a monodentate ligand (acetate, OAc^-), bidentate ligands (ethylenediamine, en; glycinate, gly^-; sarcosinate, sar^-), and a tetradentate ligand (ethylenediamine-*N*,*N*′-diacetate, $edda^{2-}$) and reaction volumes for proton dissociation of the conjugate acid of the ligands have been measured dilatometrically at 25.0 °C and I = 0.10 mol dm^{-3} ($NaClO_4$) in aqueous solution. $\Delta V°$ values (cm^3 mol^{-1}) for complex formation are as follows: 8.0 ± 1.5 ($Ni(OAc)^+$), 11.2 ± 0.2 ($Ni(gly)^+$), 12.0 ± 0.5 ($Ni(gly)_2$), 11.7 ± 0.5 ($Ni(sar)^+$), 9.9 ± 0.8 ($Ni(sar)_2$), 5.2 ± 0.5 ($Ni(en)^{2+}$), 5.6 ± 0.9 ($Ni(en)_2^{2+}$), 28.6 ± 0.2 (Ni(edda)). $\Delta V°$ values (cm^3 mol^{-1}) for proton dissociation are as follows: −10.6 ± 0.2 (HOAc), 1.4 ± 0.3 (Hgly), 0.7 ± 0.2 (Hsar), 5.6 ± 0.2 (Hen^+), 12.0 ± 0.1 (H_2en^{2+}), −0.6 ± 0.2 ($Hedda^-$), 4.9 ± 0.3 (H_2edda). The proton dissociation constants of conjugate acids of ligands and the stability constants of the nickel(II) complexes were also determined potentiometrically under the same conditions as for the dilatometric study. We discussed these reaction volumes in terms of electrostriction, contraction of donor atoms in ligands in the first coordination sphere, expansion of complexes by bond elongation due to bound ligands, and "volume chelate effect" resulting from the different packing of multidentate ligands at the metal ion and in the bulk solvent.

Introduction

Recently chemical processes at high pressure have been extensively studied with developments of high-pressure techniques.[1-3] It has been proved that reaction volumes are the most useful for a better understanding of solute–solvent interactions and that the volume profile of chemical processes is very useful in mechanistic consideration.[3-9] One of our purposes is to measure reaction volumes for the formation of a series of metal complexes to provide fundamental data for the complexation in solution and to make possible prediction of the pressure effect on the complexation. For the present study we selected some nickel(II) complexes with ligands having various combination of N and O donors.

Experimental Section

Reagents. Nickel(II) perchlorate solution was prepared by the following procedure. Perchloric acid (70%) was added to a nickel(II) chloride solution, and the solution was heated to expel hydrogen chloride.

(1) Kelm, H., Ed. *High Pressure Chemistry*; Reidel: Boston, MA, 1978.
(2) Isaacs, N. S. *Liquid Phase High Pressure Chemistry*; Wiley: New York, 1981.
(3) van Eldik, R., Ed. *Inorganic High Pressure Chemistry*; Elsevier: New York, 1986.
(4) le Noble, W. J. *Rev. Phys. Chem. Jpn.* **1980**, *50*, 207.
(5) McCabe, J. R.; Grieger, R. A.; Eckert, C. A. *Ind. Eng. Chem. Fundam.* **1970**, *9*, 156.
(6) Palmer, D. A.; Kelm, H. *Coord. Chem. Rev.* **1981**, *36*, 89.
(7) Ishihara, K.; Funahashi, S.; Tanaka, M. *Inorg. Chem.* **1983**, *22*, 2564.
(8) Ishihara, K.; Funahashi, S.; Tanaka, M. *Inorg. Chem.* **1983**, *22*, 3589.
(9) Funahashi, S.; Uchiyama, N.; Ishii, M.; Tanaka, M. *Inorg. Chim. Acta* **1987**, *128*, 169.

0020-1669/88/1327-3368$01.50/0 © 1988 American Chemical Society